Interconnected Four Poles Magnetic Bearings Simulations and Testing

D. F. B. David[a], J. A. Santisteban[a], A .C. Del Nero Gomes[b]

[a] Universidade Federal Fluminense, Rua Passo da Pátria 156, 20420-240 Niteroi, Brazil, domingos@vm.uff.br
[b] Universidade Federal do Rio de Janeiro, Centro de Tecnologia, Rio de Janeiro, Brazil

***Abstract*—This article proposes and analyses a new idea to be used in magnetic bearings. It is an adaptation of a structure that has already worked successfully in split-winding self-bearing motors. Preliminary theoretical results predict that a greater equivalent stiffness could be achieved when compared with the values associated with the traditional active magnetic bearing conception in the literature.**

I. Introduction

The conventional structure of active magnetic bearings (AMBs) used with rotating machines [1][2][3], here called Type A, is shown in figure 1. It can be seen as four "U-shaped electromagnets", two of them in the x or horizontal direction and the other in the y or vertical direction, resulting in four independent magnetic flux loops .

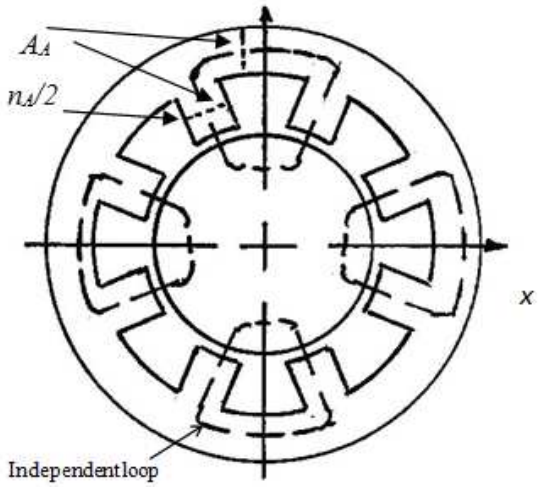

Figure 1. In type A, or traditional AMBs, the opposing pairs of windings along the x (y) direction control the horizontal (vertical) position; there are no connections among the flux paths.

The windings in the x and y direction are fed with currents $I_0 \pm i_x(t)$ and $I_0 \pm i_y(t)$; the constant DC current I_0 is the base, or bias, and the differential currents i_x and i_y will control the rotor position. Using basic reluctance concepts, the resultant forces f_x and f_y can be expressed in terms of these currents, the air magnetic permeability μ_0, the total number of coils n_a, the cross section area in the static ferromagnetic material A_a and the nominal length h of the air gaps. After a standard linearization procedure [1] around the operating point $x = y = i_x = i_y = 0$, the forces generated by the type A structure are shown in (1). Notice that the non connected nature of the magnetic fluxes leads to uncoupled forces.

$$\left.\begin{array}{l} f_x = k_p^a x + k_i^a i_x \\ f_y = k_p^a y + k_i^a i_y \end{array}\right\} \text{ where } \left\{\begin{array}{l} k_p^a = \mu_0 A_a n_a^2 I_0^2/h^3 \\ k_i^a = \mu_0 A_a n_a^2 I_0/h^2 \end{array}\right. \quad (1)$$

An alternative structure for magnetic bearings, here named Type B, is possible; it contains four windings but now with interconnected magnetic loops, as depicted in figure 2. This structure is found in the split-windings self-bearing motors researched in Brazil [4],[5]. In that approach, to provide a simultaneous torque, alternate currents are injected in the windings; in AMBs, continuous currents are considered.

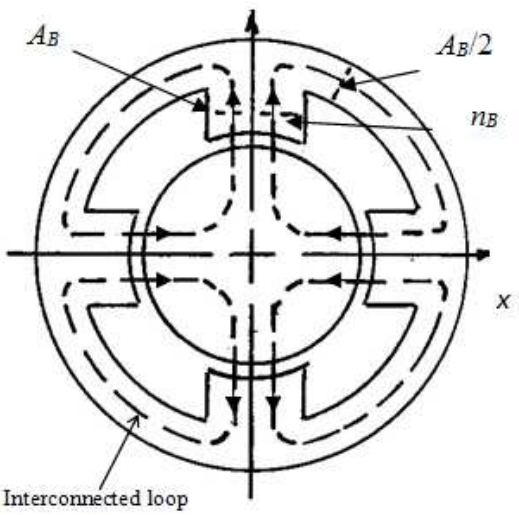

Figure 2. In type B, the proposed AMBs, even though the flux paths are interconnected, the control currents in coils along the x (y) direction affect only that horizontal (vertical) direction.

The generation of reluctance forces in Type B is presented in section II. The resulting linearized expressions also show a decoupled nature, and the position and current constants, k_p^b and k_i^b, have higher values than in the A case. Section III presents analytical results and simulations on how increasing $k_{p,i}^b$ affects dynamic and control aspects of AMBs. Discussions about tests, final comments and considerations on what remains to be done are made in sections IV and V.

The authors wish to thank FAPERJ for the financial support

Although other results are known with the Type B bearing concept [6], the authors of this article did not identify, up to the present time, the association of its interconnected structure with uncoupled equations for radial restoring forces or with higher values of the magnetic constants.

II. Reluctance Forces in Type B Bearings

A detailed study of the force generation was presented in [4] and in [7]; the main points are repeated below. The x and y components of a radial displacement of the rotor change the nominal gap width h as shown in figure 3.

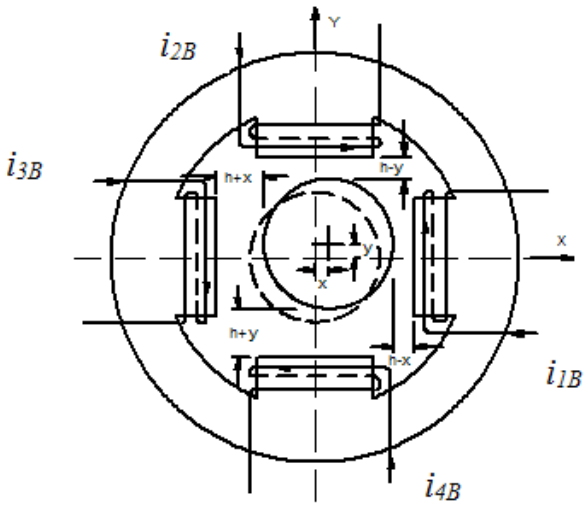

Figure 3. When the rotor moves x and y in the horizontal and vertical positions, the air gap widths change to $h - x$ in the right pole, $h + x$ (left pole), $h - y$ (upper pole) and $h + y$ (lower pole).

The usual procedure to compensate the displacements is the application of differential currents [1] to the pairs of windings: the differential, or control, currents $i_x(t)$, for the x or horizontal direction, and $i_y(t)$, for the vertical direction, are added an subtracted to a base, or bias, current I_0, a constant DC level. The total currents, neglecting the index $_B$ appearing in figure 3, imposed at each winding are

$$i_1(t) = I_0 + i_x(t),\ i_3(t) = I_0 - i_x(t) \quad \text{for the } x \text{ direction} \tag{2}$$

$$i_2(t) = I_0 + i_y(t),\ i_4(t) = I_0 - i_y(t) \quad \text{for the } y \text{ direction} \tag{3}$$

Dotted lines in figure 2 represent the magnetic flux distribution caused by these currents. The reluctance forces depend on the magnetic fluxes ϕ_k, $k = 1, 2, 3, 4$, in the four air gaps with cross section A_b:

$$f_x = \frac{\phi_1^2 - \phi_3^2}{2\mu_0 A_b} \quad \text{and} \quad f_y = \frac{\phi_2^2 - \phi_4^2}{2\mu_0 A_b} \tag{4}$$

Due to the ferromagnetic connections in type B, a current injected in any winding will cause fluxes in all four air gaps; figure 4 illustrates the effects of i_1 in all four "poles". If ϕ_{jk} denotes the flux in air gap j caused by a current in winding k, the total magnetic flux ϕ_1 in "pole" 1 is a function of the fluxes $\phi_{11}, \phi_{12}, \phi_{13}, \phi_{14}$. Assuming no air or ferromagnetic losses, and positive signs for fluxes headed to the rotating center, the total magnetic fluxes in the poles are:

$$\phi_1 = \phi_{11} + \phi_{12} - \phi_{13} + \phi_{14}. \tag{5}$$

$$\phi_2 = -\phi_{21} - \phi_{22} - \phi_{13} + \phi_{24} \tag{6}$$

$$\phi_3 = -\phi_{31} + \phi_{32} - \phi_{13} + \phi_{34} \tag{7}$$

$$\phi_4 = -\phi_{14} + \phi_{42} - \phi_{13} - \phi_{44}. \tag{8}$$

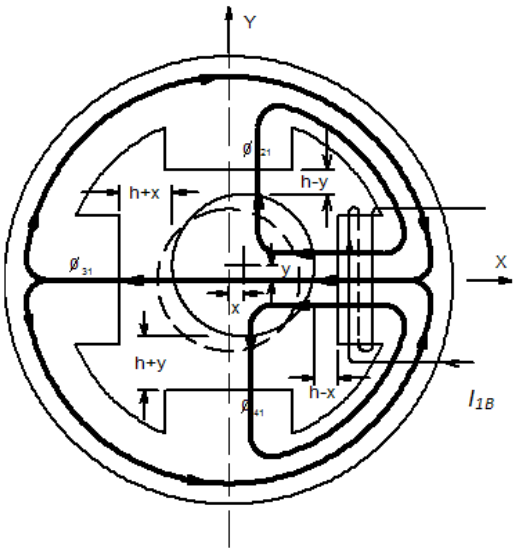

Figure 4. Magnetic flux distribution associated to i_1 in type B magnetic bearing; current injected only in winding 1 causes fluxes in all air gaps.

For the determination of the sixteen values of ϕ_{jk}, let the magneto-motive force generated by current i_1 be denoted by $\mathcal{F}_1$, and the reluctances of the air gaps in the four poles in figure 3 by $\mathcal{R}_1$, $\mathcal{R}_2$, $\mathcal{R}_3$ and $\mathcal{R}_4$. Figure 5 shows the equivalent magnetic circuit.

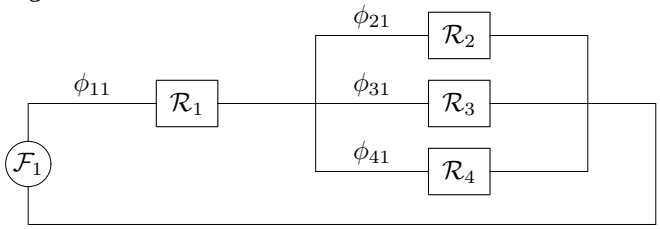

Figure 5. Magnetic flux equivalent circuit associated to current only in winding 1 of type B magnetic bearing.

In the following development, A_b is the cross section area of the poles in figure 2. Considering that the reluctances are

$$\mathcal{R}_1 = \frac{h-x}{\mu_0 A_b}, \mathcal{R}_2 = \frac{h-y}{\mu_0 A_b}, \mathcal{R}_3 = \frac{h+x}{\mu_0 A_b}, \mathcal{R}_4 = \frac{h+y}{\mu_0 A_b}, \tag{9}$$

the equivalent reluctance $\mathcal{R}_1^e$ can be found to be

$$\mathcal{R}_1^e = \frac{\mathcal{R}_1\mathcal{R}_2\mathcal{R}_3 + \mathcal{R}_1\mathcal{R}_2\mathcal{R}_4 + \mathcal{R}_1\mathcal{R}_3\mathcal{R}_4 + \mathcal{R}_2\mathcal{R}_3\mathcal{R}_4}{\mathcal{R}_2\mathcal{R}_3 + \mathcal{R}_2\mathcal{R}_4 + \mathcal{R}_3\mathcal{R}_4}. \tag{10}$$

To avoid cumbersome formulas, the auxiliary variables are defined

$$N = \mathcal{R}_1\mathcal{R}_2\mathcal{R}_3 + \mathcal{R}_1\mathcal{R}_2\mathcal{R}_4 + \mathcal{R}_1\mathcal{R}_3\mathcal{R}_4 + \mathcal{R}_2\mathcal{R}_3\mathcal{R}_4, \tag{11}$$

$$D_1 = \mathcal{R}_2\mathcal{R}_3 + \mathcal{R}_2\mathcal{R}_4 + \mathcal{R}_3\mathcal{R}_4, \quad (12)$$

$$D_2 = \mathcal{R}_1\mathcal{R}_3 + \mathcal{R}_1\mathcal{R}_4 + \mathcal{R}_3\mathcal{R}_4, \quad (13)$$

$$D_4 = \mathcal{R}_1\mathcal{R}_2 + \mathcal{R}_1\mathcal{R}_4 + \mathcal{R}_2\mathcal{R}_4, \quad (14)$$

$$D_4 = \mathcal{R}_1\mathcal{R}_2 + \mathcal{R}_1\mathcal{R}_3 + \mathcal{R}_2\mathcal{R}_3. \quad (15)$$

Since $\mathcal{F}_1 = n_b i_1$, algebraic operations lead to the following expressions for the magnetic fluxes associated to current $i_1 = I_0 + i_x$ imposed to the winding in pole 1 of figure 3:

$$\phi_{11} = \frac{\mathcal{F}_1}{\mathcal{R}_1^e} = n_b(I_0 + i_x)\frac{D_1}{N}, \quad (16)$$

$$\phi_{21} = n_b(I_0 + i_x)\frac{\mathcal{R}_3\mathcal{R}_4}{N}, \quad (17)$$

$$\phi_{31} = n_b(I_0 + i_x)\frac{\mathcal{R}_2\mathcal{R}_4}{N}, \quad (18)$$

$$\phi_{41} = n_b(I_0 + i_x)\frac{\mathcal{R}_2\mathcal{R}_3}{N}. \quad (19)$$

The same procedure, repeated for currents i_2, i_3, i_4 imposed at the windings in poles 2, 3 and 4 in figure 3, results in

$$\phi_{12} = n_b(I_0 + i_y)\frac{\mathcal{R}_3\mathcal{R}_4}{N} \quad \phi_{22} = n_b(I_0 + i_y)\frac{D_2}{N}$$

$$\phi_{32} = n_b(I_0 + i_y)\frac{\mathcal{R}_1\mathcal{R}_4}{N} \quad \phi_{42} = n_b(I_0 + i_y)\frac{\mathcal{R}_1\mathcal{R}_3}{N}$$

$$\phi_{13} = n_b(I_0 - i_x)\frac{\mathcal{R}_2\mathcal{R}_4}{N} \quad \phi_{23} = n_b(I_0 - i_x)\frac{\mathcal{R}_1\mathcal{R}_4}{N}$$

$$\phi_{33} = n_b(I_0 - i_x)\frac{D_3}{N} \quad \phi_{43} = n_b(I_0 - i_x)\frac{\mathcal{R}_1\mathcal{R}_2}{N}$$

$$\phi_{14} = n_b(I_0 - i_y)\frac{\mathcal{R}_2\mathcal{R}_3}{N} \quad \phi_{24} = n_b(I_0 - i_y)\frac{\mathcal{R}_1\mathcal{R}_3}{N}$$

$$\phi_{34} = n_b(I_0 - i_y)\frac{\mathcal{R}_1\mathcal{R}_2}{N} \quad \phi_{44} = n_b(I_0 - i_y)\frac{D_4}{N}$$

The total fluxes ϕ_k for $k = 1, 2, 3, 4$ can be determined by substituting the previous values of the partial fluxes ϕ_{jk} in equations (5) to (8). Then, with the help of (4), the total reluctance forces generated in a type B magnetic bearing can be expressed as

$$f_x = \frac{\mu_0 A_b n_b^2}{2} q_x(h, x, y, I_0, i_x, i_y) \quad (20)$$

$$f_y = \frac{\mu_0 A_b n_b^2}{2} q_y(h, x, y, I_0, i_x, i_y) \quad (21)$$

where $q_{x,y}$ are complicated functions of their arguments:

$$q_x(h, x, y, I_0, i_x, i_y) = \frac{N_1^2 - N_2^2}{\Delta^2} \quad (22)$$

$$q_y(h, x, y, I_0, i_x, i_y) = \frac{N_3^2 - N_4^2}{\Delta^2} \quad (23)$$

with

$$N_1 = i_1\Delta_1 + i_2\Delta_2 - i_3\Delta_3 + i_4\Delta_4$$

$$N_2 = i_3\Delta_5 - i_1\Delta_3 + i_2\Delta_6 + i_4\Delta_7$$

$$N_3 = -i_2\Delta_1 - i_3\Delta_2 - i_1\Delta_3 + i_4\Delta_8$$

$$N_4 = -i_4\Delta_5 + i_1\Delta_3 + i_2\Delta_8 + i_3\Delta_7.$$

The currents i_k are defined in equations (2) and (3); if the distances $h \pm x$ and $h \pm y$ are denoted by $\delta_x^{\pm}$ and $\delta_y^{\pm}$, the Δs above are

$$\Delta_1 = \Delta_2 + \Delta_3 + \Delta_4,\ \Delta_2 = \delta_x^+\delta_y^+,\ \Delta_3 = \delta_y^+\delta_y^-,\ \Delta_4 = \delta_x^+\delta_y^-$$

$$\Delta_5 = \Delta_3 + \Delta_6 + \Delta_7,\ \Delta_6 = \delta_x^-\delta_y^+,\ \Delta_7 = \delta_x^-\delta_y^-,\ \Delta_8 = \delta_x^+\delta_x^-$$

$$\Delta = \delta_x^-\delta_y^-\delta_x^+ + \delta_x^-\delta_y^-\delta_y^+ + \delta_x^-\delta_x^+\delta_y^+ + \delta_y^-\delta_x^+\delta_y^+$$

The complexity of the above formulas makes the linearization of (20) and (21) a hard task. Considering that the AMB operates around a point $P_0 = (x, y, i_x, i_y)_0 = (0, 0, 0, 0)$, the use of symbolical computation allows the calculation of the partial derivatives:

$$\left.\frac{\partial q_x}{\partial x}\right|_{P_0} = \frac{4I_0^2}{h^3} \qquad \left.\frac{\partial q_x}{\partial y}\right|_{P_0} = 0 \quad (24)$$

$$\left.\frac{\partial q_x}{\partial i_x}\right|_{P_0} = \frac{4I_0}{h^2} \qquad \left.\frac{\partial q_x}{\partial i_y}\right|_{P_0} = 0. \quad (25)$$

If a similar procedure is made for q_y, the combined results lead to the linear expressions for the type B structure forces:

$$\left.\begin{aligned} f_x &= k_p^b x + k_i^b i_x \\ f_y &= k_p^b y + k_i^b i_y \end{aligned}\right\} \text{where} \left\{\begin{aligned} k_p^b &= 2\mu_0 A_b n_b^2 I_0^2/h^3 \\ k_i^b &= 2\mu_0 A_b n_b^2 I_0/h^2 \end{aligned}\right. \quad (26)$$

Two remarkable aspects are to be noted: (a) even though the fluxes are interconnected in a type B structure, the forces are decoupled, exactly as they were in type A; (b) a factor 2 appears in the formulas above.

III. Theoretical Evaluations and Simulations

Assuming the same outside diameter of the stator, the following advantages can be identified for the Type B active magnetic bearing when it is compared with Type A:

1) The position and current constants k_p^b and k_i^b in (26) are two times bigger than their counterparts k_p^a and k_i^a in equation (1);
2) the cross section area A_b can be chosen greater than A_a; it is reasonable to have $A_b \approx 2A_a$;
3) the number of coils n_b can, possibly, be larger than n_a.

The net conclusion is: the position (k_p) and current (k_i) constants for Type B AMBs have values 2 times higher than in case A. Depending on design aspects (A_b and n_b), even higher rates can be achieved. How much can these constants be increased? The magnetic saturation seems to be the limit.

To evaluate the effects of k_b and k_i in an AMB performance, consider the problem, illustrated in figure 6, of positioning a particle of mass m that moves without friction in a horizontal, rectilinear path.

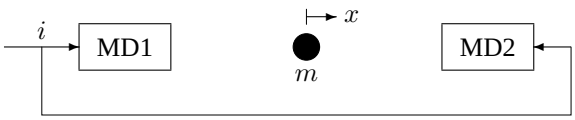

Figure 6. The mass position $x(t)$ is to be controlled by the magnetic devices.

The magnetic devices MD1 and MD2 apply a (horizontal) force $f(t) = k_p x(t) + k_i i(t)$ on the sphere, where i is a control

current and x measures the displacement with respect to the reference position. A controller is desired, capable of driving the sphere position $x(t)$ to 0 for all possible initial conditions $x(0)$, and in the eventual presence of constant, horizontal disturbance forces d. This is a simple, but meaningful, problem: many theorectical aspects of the real life operation and control of AMBs are present in it.

A mathematical model is found, after a simple application of Newton's laws: $f(t)+d(t) = m\ddot{x}(t)$. The linear nature of f leads to $m\ddot{x}(t)-k_p x(t) = k_i i(t)+d(t)$, or $(ms^2-k_p)X(s) = k_i I(s) + D(s)$. A block diagram is

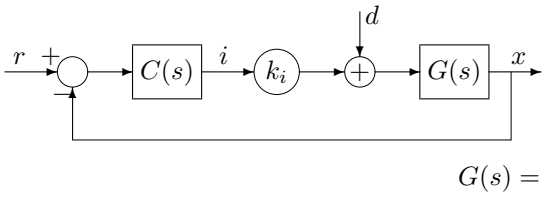

Figure 7. Block diagram showing the plant dynamics and a closed loop control scheme with a controller $C(s)$.

A stabilizing PD controller $C(s) = \alpha s+\beta$ can be designed; it guarantees that initial displacements $x(0) \neq 0$ are corrected, when $d = 0$. The speed of convergence of $x(t)$ depends on the adjustable location of the closed loop poles, which is a function of the controller parameters α and β.

The effects of extra forces d on the sphere position can be evaluated by the expression $X(s) = T_d(s)D(s)$, where the disturbance transfer function $T_d(s)$ can be obtained from the above diagram, assuming $r = 0$:

$$T_d(s) = \frac{G(s)}{1 + k_i G(s)C(s)} = \frac{1/m}{s^2 + a_1 s + a_0}$$

where the characteristic polynomial coefficients are

$$a_1 = \frac{\alpha k_i}{m} \qquad \text{and} \qquad a_0 = \frac{\beta k_i - k_p}{m}.$$

The steady state influence of disturbances in the sphere position can be measured by $\rho = \lim x(t)$ when $t \to \infty$, when $r = 0$. Assuming closed loop stability, the Final Value Theorem can be used, and

$$\rho = \lim_{t\to\infty} x(t) = \lim_{s\to 0} sX(s) = \lim_{s\to 0} sT_d(s)D(s)$$

But, for constant disturbances, $D(s) = d_0/s$ leading to

$$\rho = \lim_{s\to 0} sT_d(s)\frac{d_0}{s} = d_0 T_d(0) = \frac{d_0}{\beta k_i - k_p} \qquad (27)$$

The well known fact that PD controllers do not completely reject ($\rho = 0$) constant disturbances becomes aparent. But equation (27) tells more: for a fixed, stabilizing controller, ρ decreases when k_p and k_i increase by the same factor.

In other words, if the position and current coefficients in a magnetic force generation law are both increased by the same amount, the resulting PD control is less sensitive to constant disturbances, and this characterizes a better, stiffer suspension.

Since a full, steady state rejection of constant disturbances can be achieved by PID controllers, consider now $C(s) = \alpha s+\beta+\gamma/s$. The new disturbance transfer function $T_d(s)$ is

$$T_d(s) = \frac{s/m}{s^3 + a_2 s^2 + a_1 s + a_0} \text{ with } \begin{cases} a_2 = \alpha k_i/m \\ a_1 = (\beta k_i - k_p)/m \\ a_0 = \gamma k_i/m \end{cases}$$

Because each coefficient depends on a single controller parameter, the closed loop poles can be arbitrarily assigned, thus ensuring stability. A simple calculation would show that complete rejection ($\rho = 0$) of step disturbances is indeed achieved by the PID controller.

In order to feel the performance details of the situation, a simulation was performed. The numerical values, in the SI system, $m = 4$, $k_i^0 = 200$ and $k_p^0 = 2000000$ were used. A PID controller that assigns all the closed loop poles at -10 was calculated: $\alpha = 3/5$, $\beta = 10006$ and $\gamma = 20$.

An initial displacement of 1cm was imposed to the sphere, and in less than 1 second it returned to the desired rest position $x = 0$. After stabilization, a constant disturbance ($d_0 = 40$N) was applied and successfully rejected. Figure 8 shows the curves for different values of the k_i and k_p constants: (k_i^0, k_p^0), $(2k_i^0, 2k_p^0)$, $(4k_i^0, 4k_p^0)$ and $(8k_i^0, 8k_p^0)$.

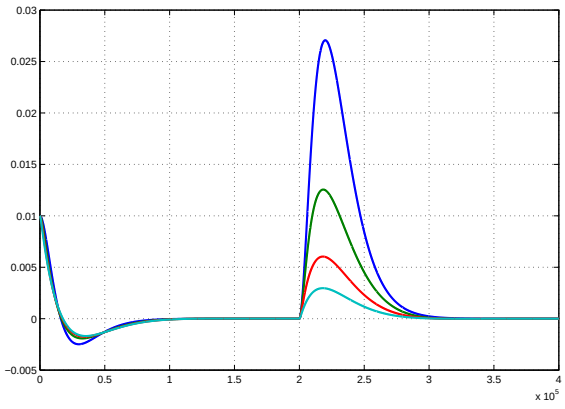

Figure 8. Sphere positioning with PID control for several values of the magnetic constants k_p and k_i. The highest rising, dark blue curve refers to the nominal values (NV) k_p^0 and k_i^0; twice the NV leads to the dark green (second highest rising) curve; four and eight times the NV generate the next curves, red and light blue. Total simulation time: 4s, displacements in meters.

All curves are very similar in the first 2 seconds, implying that high or low values for the magnetic constants are not crucial in the stabilizing stage. But when constant disturbance rejection is needed, better transient behaviours are a direct consequence of higher values in k_p and k_i.

It is important to stress, again, that this is a simple example, but the conclusions allowed by it are valid in much more general situations, involving real world applications of practical interest. And these conclusions are: increasing the values of the magnetic force constants k_p and k_i is a highly desirable goal in the AMB field.

IV. Prototype Testing

Section II final conclusions are that the interconnected fluxes in the type B structure increase the values of the

magnetic force constants k_p and k_i. How sure can one be about the theoretical tools used in those developments? Are the symbolical algebra calculations safe?

It is our understanding that the idea of the Type B structure has already been tested. In fact, in the prototype used at UFRJ [4], a vertical rotor is radially positioned by a self-bearing motor based on the interconnected fluxes of the type B structure. Such a situation is more complicated, because the windings are fed with AC currents, to achieve the dual capabilities: torque generation and radial positioning. And the device has worked!

The best possible way to give definite answers to the seminal questions posted in the beginning of this section is by constructing prototypes and testing them in an exhaustive way. Only after this important stage, will the ideas proposed here be validated. Or not.

Some steps have already been walked in that direction: a pair of prototypes, one for type A and the other for type B, are under construction. Figures 9 and 10 show their geometries.

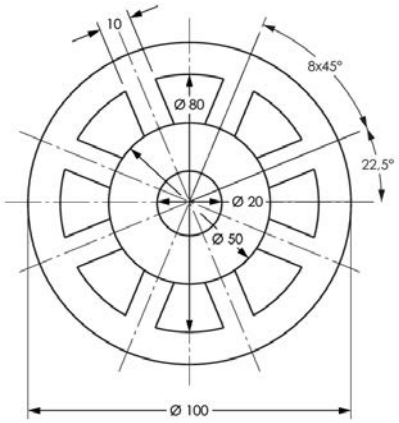

Figure 9. Type A magnetic bearing geometry.

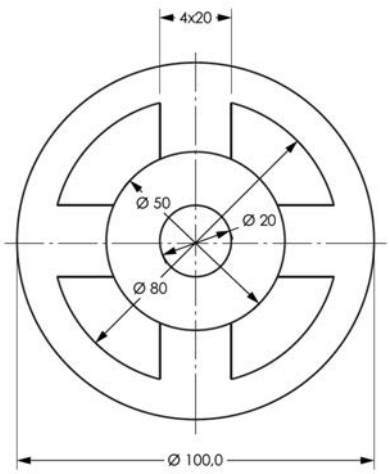

Figure 10. Type B magnetic bearing geometry.

They will be applied to a vertical rotor driven by a two-phase induction motor; the lower support will be provided by a mechanical bearing. Figure 11 shows these ideas.

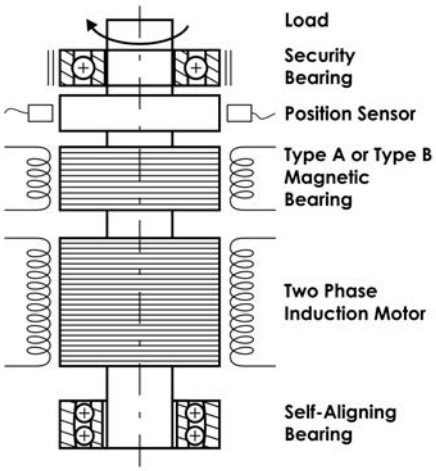

Figure 11. Testing prototype concept.

A finite element simulation of the magnetic characteristics of type A and type B structures was done, and some results are shown below.

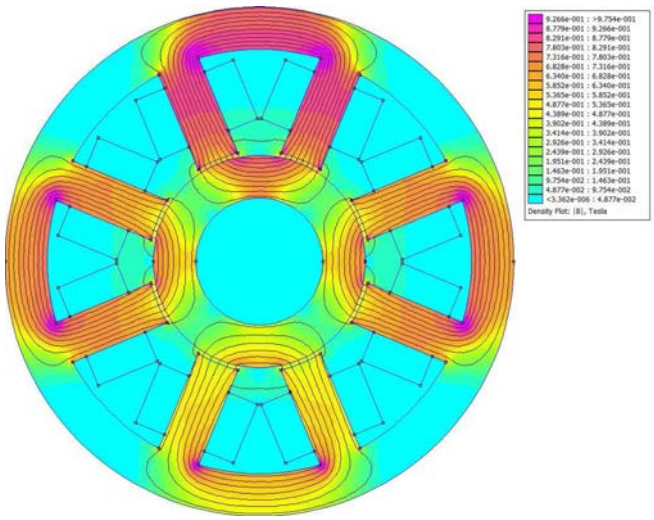

Figure 12. Flux distribution in a type A structure with balanced currents in the x axis and a differential current in the y direction.

Figure 13 shows clearly that a differential current in one direction does not affect the flux distribution in the other direction, thus confirming equation (25).

V. Final Comments and Conclusions

The authors have great expectations that the here called type B concept will be a valid contribution for the active magnetic bearings field, because of the possibility of increasing their equivalent mechanical stiffness.

References

[1] G. Schweitzer, H. Bleuler, and A. Traxler, *Active Magnetic Bearings*. Hochshulverlag AG an der ETH Zürich, 1994.

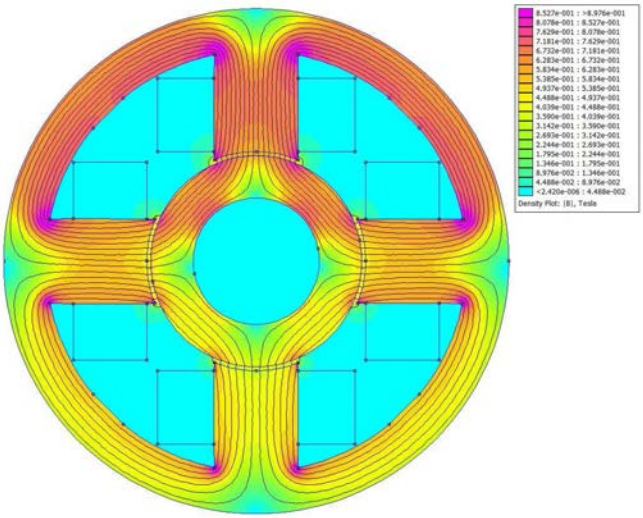

Figure 13. Flux distribution in a type B structure with balanced currents in the x axis and a differential current in the y direction.

[2] A. Chiba, T. Fukao, O. Ichikawa, M. Oshima, M. Takemoto, and D. Dorrell, *Magnetic Bearings and Bearingless Drives*. Newnes-Elsevier, 2005.

[3] G. Schweitzer, E. Maslen, H. Bleuler, M. Cole, P. Keogh, R. Larsonneur, R. Nordmann, and Y. Ogada, *Magnetic Bearings: Theory, Design and Applications to Rotating Machinery*. Springer-Verlag, 2009.

[4] D. F. B. David, "Levitação de rotor por mancais-motores radiais magnéticos e mancal axial sc auto-estável," D. Sc. tese, COPPE–UFRJ, 2000.

[5] E. F. Rodriguez and J. A. Santisteban, "An improved control system for a split winding bearingless induction motor," *IEEE Transactions on Industrial Electronics*, vol. 58, no. 8, pp. 3401–3408, 2011.

[6] L. Santos and K. Kjolhed, "Experimental contribution to high-precision characterization of magnetic forces in active magnetic bearings," *Journal of Engineering for Gas Turbines and Power*, vol. 129, pp. 503–, 2007.

[7] D. F. B. David, J. A. Santisteban, and A. C. D. N. Gomes, "Interconnected four poles magnetic bearings," in *Proceedings of the 1st Brazilian Workshop on Magnetic Bearings*, www.magneticbearings2103.com.br, october 2013.